

Electronic Supplementary Information

Flexible Dielectric Papers Based on Biodegradable Cellulose Nanofibers and Carbon Nanotubes for Dielectric Energy Storage

Xiaoliang Zeng^{a,b}, Libo Deng^c, Yimin Yao^{a,b}, Fangfang Wang^a, Rong Sun^{a,}, Jianbin Xu^{d,*}, and Ching-Ping Wong^{d,e}*

^aShenzhen Institute of Advanced Technology, Chinese Academy of Sciences, Shenzhen, 518055, China. E-mail: rong.sun@siat.ac.cn

^bShenzhen College of Advanced Technology, University of Chinese Academy of Sciences, Shenzhen, 518055, China.

^cCollege of Chemistry and Environmental Engineering, Shenzhen University, Shenzhen 518060, China

^dDepartment of Electronics Engineering, The Chinese University of Hong Kong, 999077, Hong Kong, China. E-mail: jbxu@ee.cuhk.edu.hk

^eSchool of Mechanical Engineering, Georgia Institute of Technology, 771 Ferst Drive, Atlanta, Georgia 30332, United States.

Contents

Fig. S1. (a) Atomic force microscopy image of the CNFs. (b) Diameter distribution of the CNFs.

Fig. S2. Optical image of CNF/CNT water solution (left) and CNT water solution (right) after sonication for 24 h.

Fig. S3. (a) Optical image of pure CNF paper showing high optical transparency. (b) UV-vis transmittance spectra of the CNF/CNT papers with different CNT loadings.

Fig. S4. (a) SEM surface morphological micrograph, and (b) a magnified image of common A4 paper.

Fig. S5. Dielectric constant of CNF/BaTiO₃ paper with different BaTiO₃ loadings.

Fig. S6. Schematic *P-E* loop of a dielectric material with the discharged energy density represented by the area colored in green.

Fig. S7. Linear relationship between Log (*E*) and Log (-ln (1-P(*E*))) to obtain the parameters β and E_b .

Table S1. Mechanical properties of the CNF/CNT papers with different CNT loadings.

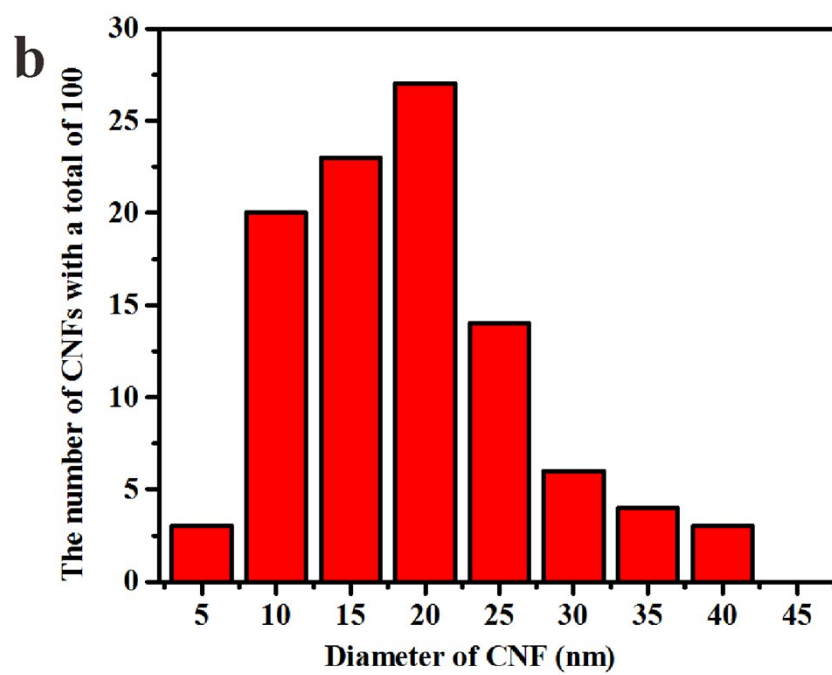
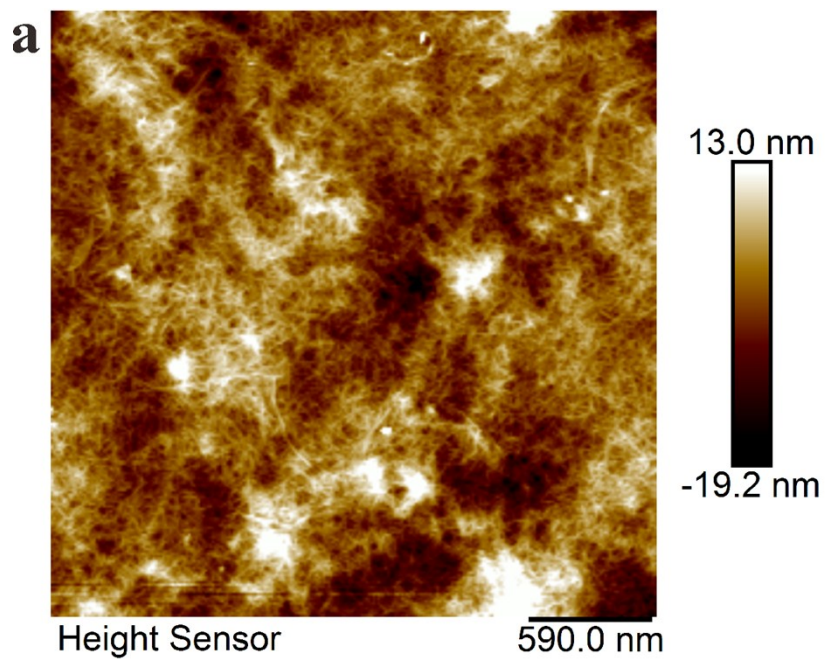


Fig. S1. (a) Atomic force microscopy image of the CNFs. (b) Diameter distribution of the CNFs.

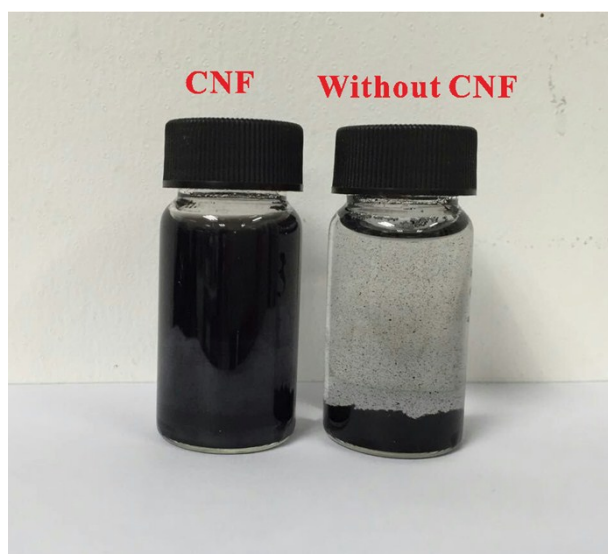


Fig. S2. Optical image of CNF/CNT water solution (left) and CNT water solution (right) after sonication for 24 h.

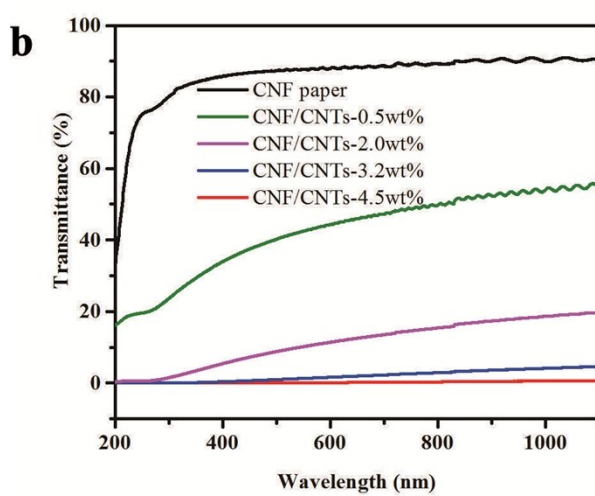


Fig. S3. (a) Optical image of pure CNF paper showing high optical transparency. (b) UV-vis transmittance spectra of the CNF/CNT papers with different CNT loadings.

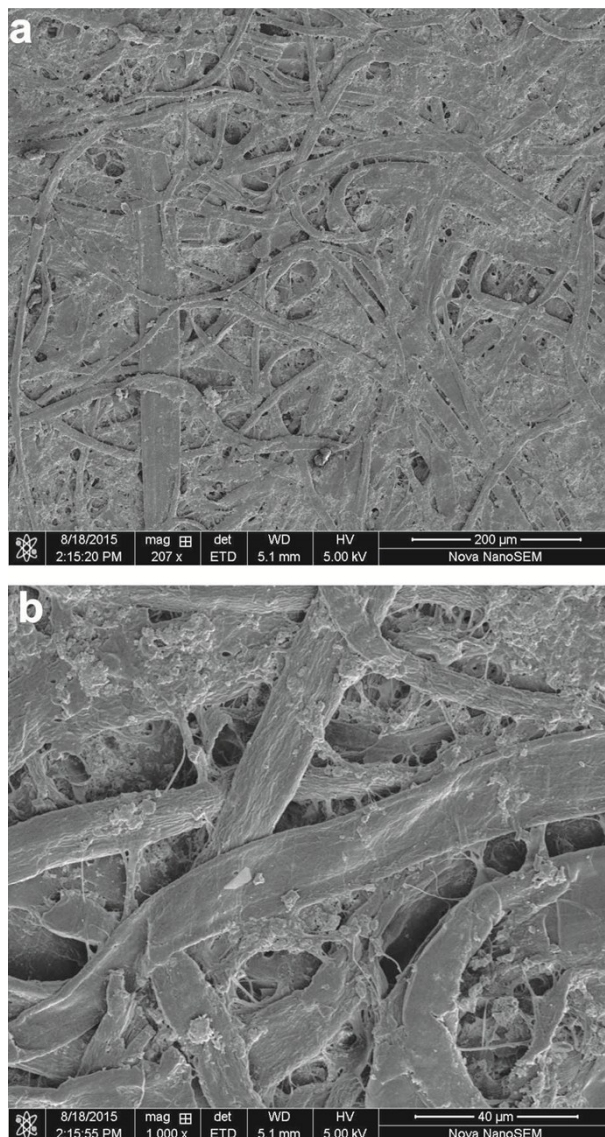


Fig. S4. (a) SEM surface morphological micrograph, and (b) a magnified micrograph of common A4 paper.

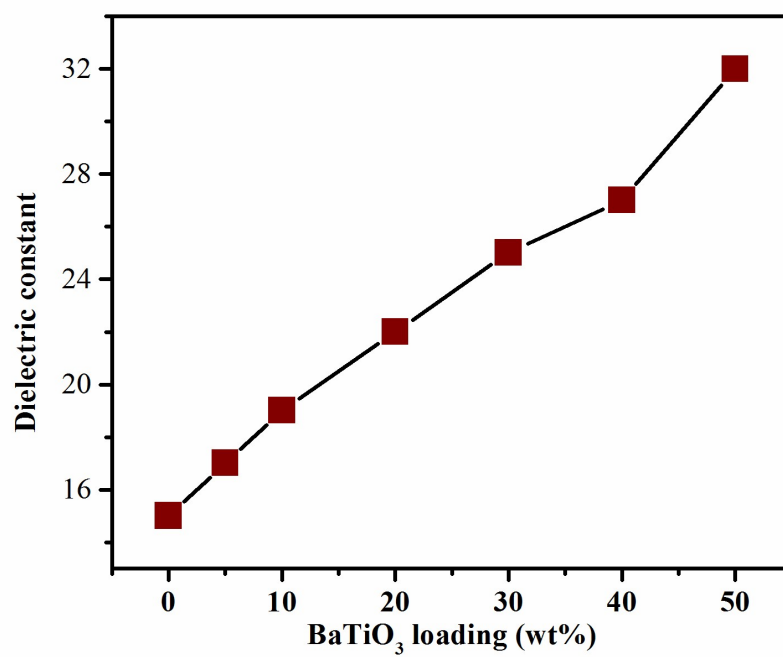


Fig. S5. Dielectric constant of CNF/BaTiO₃ paper with different BaTiO₃ loadings.

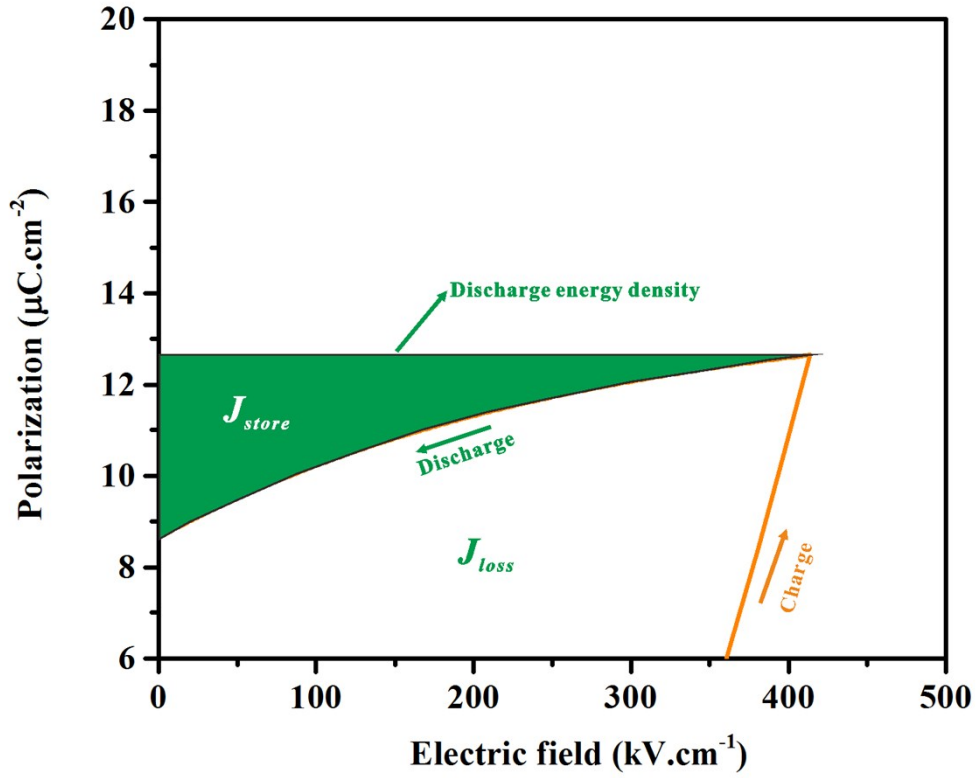


Fig. S6. Schematic P - E loop of a dielectric material with the discharged energy density represented by the area colored in green.

The energy efficiency η , can be calculated as

$$\eta = J_{store}/(J_{store} + J_{loss}) \quad (1)$$

where J_{store} and J_{loss} are energy density and energy loss, respectively, calculated from the

D - E loops in Fig. S5.

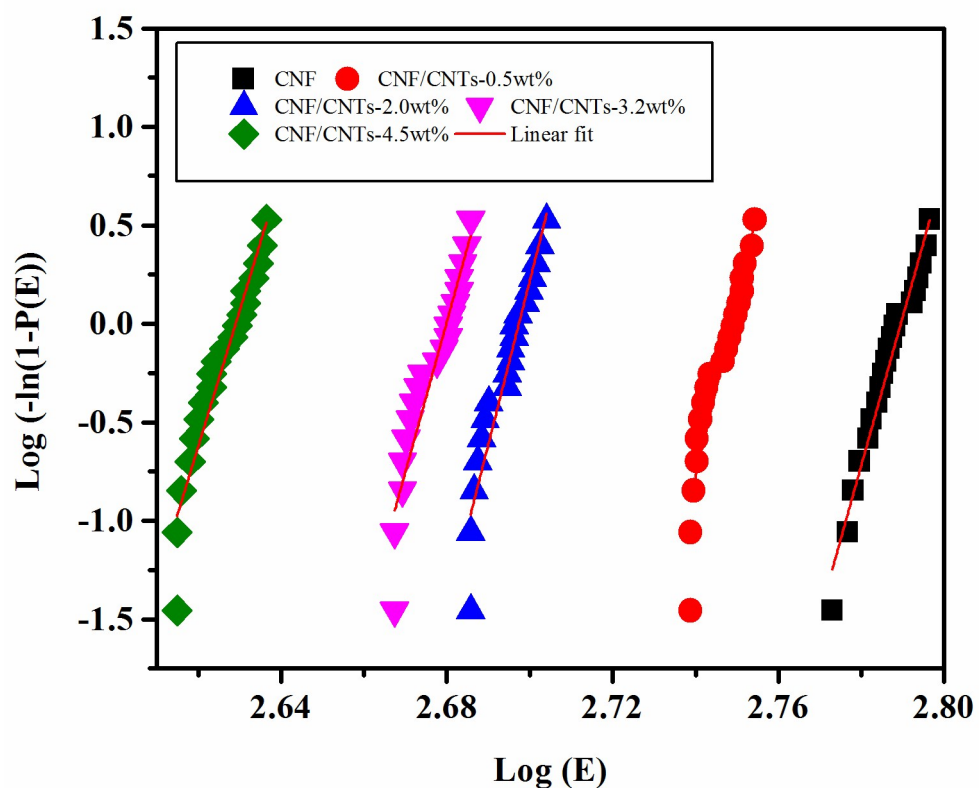


Fig. S7. Linear relationship between $\log (E)$ and $\log (-\ln (1-P(E)))$ to obtain the parameters β and E_b .

Table S1. Mechanical properties of the CNF/CNT papers with different CNT loadings.

samples	tensile Strength (MPa)	Young's modulus (GPa)	elongation (%)
CNF paper	95.0±11	6.0±1.0	2.0±0.7
CNF/CNT–0.5 wt % paper	103.6±15	7.7±0.8	1.5±1.4
CNF/CNT–2.0 wt % paper	116.7±13	8.2±0.7	2.1±0.4
CNF/CNT–3.2 wt % paper	113.3±16	6.3±1.1	3.2±0.5
CNF/CNT–4.5 wt % paper	107.5±12	5.6±0.8	3.3±0.4